AIP Applied Physics Letters

Evolution of the conductivity type in germania by varying the stoichiometry

D. R. Islamov, V. A. Gritsenko, C. H. Cheng, and A. Chin

Citation: Applied Physics Letters **103**, 232904 (2013); doi: 10.1063/1.4838297
View online: http://dx.doi.org/10.1063/1.4838297
View Table of Contents: http://scitation.aip.org/content/aip/journal/apl/103/23?ver=pdfcov
Published by the AIP Publishing

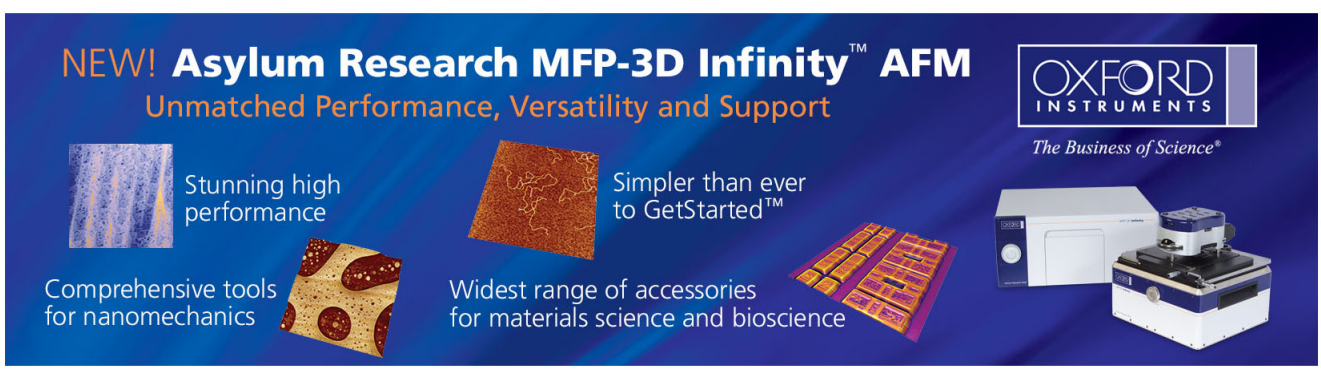

Evolution of the conductivity type in germania by varying the stoichiometry

D. R. Islamov,[1,2,a)] V. A. Gritsenko,[1,b)] C. H. Cheng,[3] and A. Chin[4,c)]
[1]*A. V. Rzhanov Institute of Semiconductor Physics, Siberian Branch of Russian Academy of Sciences, Novosibirsk 630090, Russian Federation*
[2]*Novosibirsk State University, Novosibirsk 630090, Russian Federation*
[3]*Department of Mechatronic Technology, National Taiwan Normal University, Taipei 106, Taiwan*
[4]*National Chiao Tung University, Hsinchu 300, Taiwan*

(Received 16 September 2013; accepted 17 November 2013; published online 2 December 2013)

Information regarding the conductivity type of Si/GeO_x/Ni structures with various stoichiometry has been obtained using experiments on injection of minority carriers from *n*- and *p*-type silicon. Results show that non-stoichiometric GeO_x films exhibit bipolar conductivity, that is, holes as well as electrons contribute to the charge transport. Stoichiometric GeO_2 films exhibit unipolar electron conductivity. © *2013 AIP Publishing LLC*. [http://dx.doi.org/10.1063/1.4838297]

Amorphous GeO_2 films are used as gate insulators in high mobility field effect transistors based on Ge.[1] Germania films also show resistive switching effect, which is promising for the next generation of high performance non-volatile flash memory.[2,3]

The energy diagram of the Ge/GeO_2 structure was calculated in Ref. 4, using quantum chemical simulation. According to these calculations, highly asymmetric electron and hole barriers on the Si-GeO_2 interface are predicted. The barrier for the electrons is 1.3 eV and the hole's barrier is equal to 3.2 eV. The disordered GeO_x gap value of 5.6 eV is less than the 6.1 eV calculated for crystalline germania.[5]

One of the most critical parameters of metal-oxide-silicon (MOS) structures is the sign of carriers, which contribute to the current in the insulator. The Hall effect and thermoelectric experiments cannot be performed to determine the carrier's sign in dielectrics. However, two specific methods can be used to determine the carrier's sign in the insulator. These methods are carrier sign determination in an MOS transistor,[6] and current saturation caused by non-equilibrium minority carrier generation in the depletion layer of the silicon.

Insulators can have two-band (or bipolar) conductivity, as in Si_3N_4,[6,7] HfO_2,[8] and TiO_2,[9] or monopolar charge transport (e.g., by the electrons), as in Al_2O_3,[10] and MOS with thermal SiO_2.[11] The knowledge of the carrier sign in the insulator is crucial for the interpretation of charge transport in MOS devices, as well as for the development of correct models for resistive memory switching.

In this letter, we report on the charge carrier sign determination in silicon MOS structures based on germania GeO_x.

Samples were cleaved from the wafers of Si with GeO_x film with a thickness of $d = 20$ nm. The GeO_x films were deposited using physical vapor deposition (PVD) on *p*- and *n*-type Si substrates. Samples from the first group "PDA0" were measured as deposited, that is, they were not treated using post-deposition annealing (PDA), and GeO_x films represented non-stoichiometric germania. The same GeO_x films are used in ReRAM devices.[2] The second "PDA5" and the third "PDA20" groups of samples were treated by applying PDA in an O_2 atmosphere at 300 °C for 5 min and 20 min, respectively. The 300 °C annealing is a very low temperature process for SiO_2 sublayer growing.[12] Ellipsometry measurements were user to control the thickness of GeO_x films. Structural analysis shows that the resulting GeO_x films were amorphous.

The samples for transport measurements were equipped with Ni gates of round form and a radius of 70 μm for electrical contact. Current-voltage (*J*–*V*) and capacitance-voltage (*C*–*V*) measurements were recorded at room temperature. *C*–*V* measurements were recorded at a frequency of 100 kHz. A tungsten lamp was used for light illumination. The permittivity ε was calculated from *C*–*V* measurements, using the standard formula of a flat capacitor $\varepsilon = Cd/\varepsilon_0$ in the accumulation mode, where *C* is specific capacitance and ε_0 is the electric constant (vacuum permittivity).

Figures 1(a) and 1(b) show *J*–*V* and *C*–*V* dependencies for *n*-Si/GeO_x/Ni MIS structures from the "PDA0" group for depletion and accumulation modes in the dark (solid line) and under illumination (dashed line). In accumulation mode, when a positive potential is applied to the Ni contact, almost all the applied voltage drops across the dielectric material, and the current increases exponentially with the increasing electric field. When a negative potential is applied to the metal contact, that is, in the depletion mode, the current increases exponentially at low voltages. The current saturation appears at a sufficiently large voltage, and the saturation current and its increase under illumination indicate, that in the depletion mode minority carriers are injected from Si into GeO_x. The minority carriers are holes in this case. Independent confirmations of the minority carriers injection include: (1) the existence of capacitance transition from inversion mode to non-equilibrium depletion mode, and (2) capacity increasing in non-equilibrium depletion mode under illumination (Fig. 1(b)).

Dependencies for *p*-Si/GeO_x/Ni MIS structures from the "PDA0" group for depletion and accumulation modes in the dark (solid line) and under illumination (dashed line) are shown for experimental *J*–*V* and *C*–*V* in Figs. 1(c) and 1(d), respectively. In accumulation mode, the current grows

[a)]Electronic mail: damir@isp.nsc.ru
[b)]Electronic mail: grits@isp.nsc.ru
[c)]Electronic mail: albert_achin@hotmail.com

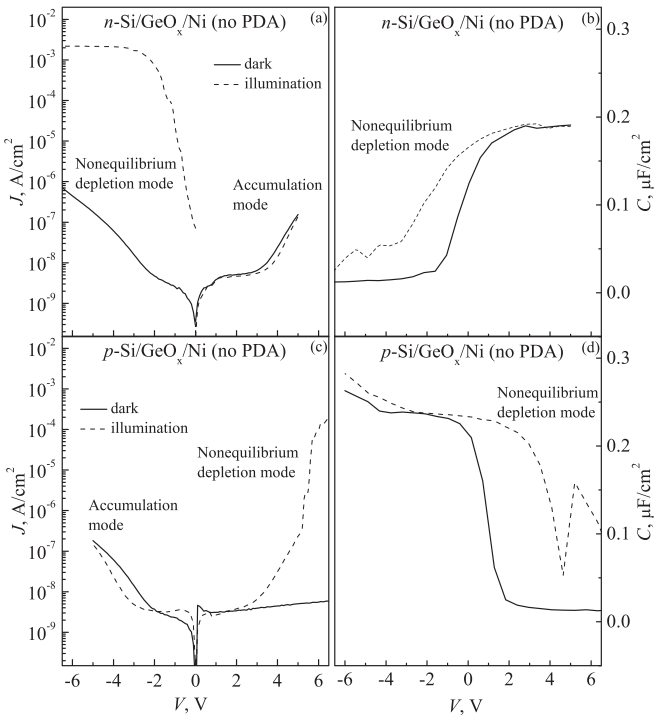

FIG. 1. Experimental *J–V* and *C–V* curves for Si/GeO$_x$/Ni MIS structures of "PDA0" group for depletion and accumulation modes in the dark (solid line) and under illumination (dashed line). (a) *J–V* and (b) *C–V* of *n*-Si/GeO$_x$/Ni structures. (c) *J–V* and (d) *C–V* of *p*-Si/GeO$_x$/Ni.

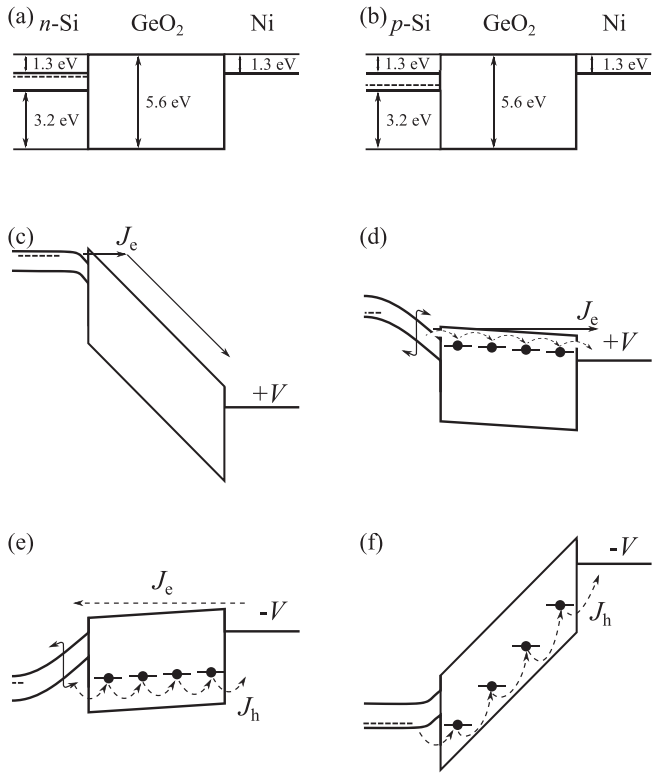

FIG. 2. Energy band diagram of *n*-Si/GeO$_2$/Ni (a) and *p*-Si/GeO$_2$/Ni (b) structures in flat band mode. The same diagrams in accumulation (c), (f), and depletion mode (d), (e). J_e/J_h are flows of injected electrons/holes from Si into GeO$_2$. Curved arrows show jumps of electrons (d) and holes (e), (f) between hole traps in the bulk of dielectric.

exponentially with increasing voltage. Current saturation appears in depletion mode, and the saturation level increases under illumination. This phenomenon indicates the injection of minority carriers, namely electrons, from the silicon substrate into germanium oxide.

The results demonstrate that GeO$_x$ conductivity is bipolar, similar to Si_3N_4,[6,7] HfO_2,[8] and TiO_2.[9]

Energy band diagrams of *n*, *p*-Si/GeO$_2$/Ni structures, based on calculations of GeO$_2$ electronic band structure,[2,4] are shown in Fig. 2 in flat band mode (Figs. 2(a) and 2(b)), in accumulation mode (Figs. 2(c) and 2(f)), and depletion mode (Figs. 2(d) and 2(e)). It is shown that the barrier for holes in the Si/GeO$_2$ interface is much higher than the barrier for electrons. Thus, it is expected that the transport in GeO$_2$ is unipolar. The difference of theoretical expectations from experimental results might be explained by one of two hypotheses. The first is based on the assumption that GeO$_x$ films are not pure GeO$_2$, and have different energy structures, that is, the energy barrier for holes in experiments is less than that in calculations. This difference increases injection probability of the holes from the Si substrate into the dielectric medium. The second hypothesis assumes that GeO$_x$ films exhibit hopping conductivity of the holes between hole traps far from the top of the valence band in the middle of the gap. If the trap density is sufficiently high, the holes hop inside of the band gap, as shown in Figs. 2(e) and 2(f).[13]

To investigate evolution of the trap density, *J–V* and *C–V* dependencies were measured for Si/GeO$_2$/Ni MIS structures after low PDA. The samples of Si/GeO$_2$/Ni after 5 min of PDA present the same behavior as with no PDA. The conductivity of the samples from "PDA5" group is bipolar.

Further PDA procedures led to the disappearance of current and capacity changes under illumination in *n*-Si/GeO$_x$/Ni structures as shown in Figs. 3(a) and 3(b): the capacitance depletion cannot be observed after annealing germania. Despite the dark current is increased, addition photocurrent is not observed in depletion mode. This phenomenon shows that injection of the minority carriers (holes) from Si into GeO$_x$ is suppressed. However, non-equilibrium depletion mode can be observed in *p*-Si/GeO$_x$/Ni structures (Figs. 3(c) and 3(d)). These phenomena show that after 300 °C O_2 annealing for long periods, the conductivity of GeO$_x$ evolves from bipolar to unipolar, namely, electronic conduction. In addition, the anomalous capacitance hump shown in Fig. 1(d), which is caused by the existence of deep interface traps, can be eliminated using oxygen annealing for periods longer than 20 min. The capacitance change in accumulation mode after anneal might be caused by the following reasons: (1) densification of poor quality GeO$_x$ (thickness decrease), (2) growing of SiO_2 sublayer, and (3) GeO$_x$ oxidation and changing of GeO$_x$ dielectric constant. Ellipsometry measurements demonstrated that the thickness of GeO$_x$ films with an accuracy of 2% has not changed after PDA. Small thickness increasing took place due to longer Ge–O (than Ge–Ge) bonds were formed by extra O in GeO$_x$ bulk. Additional SiO_2 sublayer should decrease total capacitance of Si/SiO_2/GeO$_x$/Ni structures. However, the capacitance increase is observed. The higher dielectric constant $\varepsilon_0 = 13$–14 (compared with 4–5 for samples of the "PDA0" and "PDA5" groups) and a low interface state indicates that the well-oxidized GeO$_2$ can be obtained after 300 °C O_2 annealing for 20 min. These facts

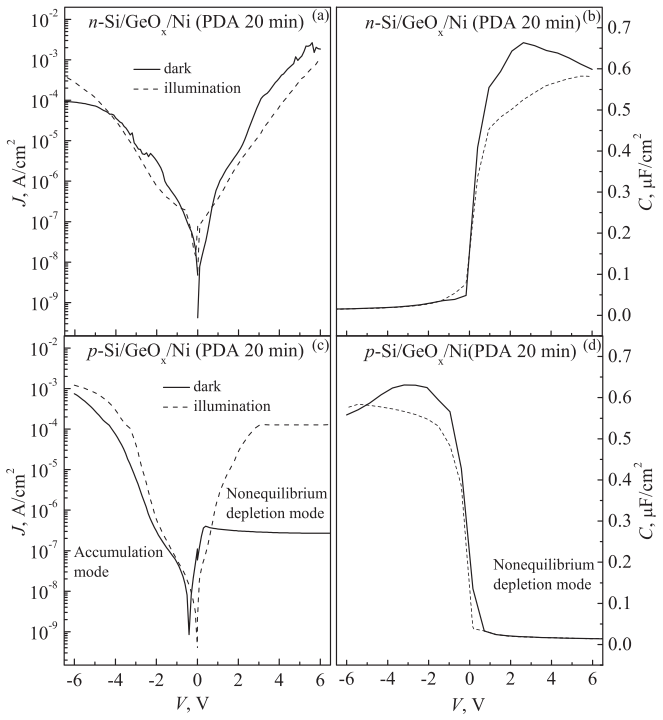

FIG. 3. Experimental *J–V* (a) and *C–V* (b) curves for *n*-Si/GeO_x/Ni MIS structures after 20 min PDA at 300 °C ("PDA20" samples group) in the dark (solid line) and under illumination (dashed line). The depletion mode is not observed in these structures. Experimental *J–V* (c) and *C–V* (d) curves for *p*-Si/GeO_x/Ni MIS structures annealed at the same conditions.

confirm both hypotheses regarding the difference in the energy structures of deposited GeO_x films and pure GeO_2, and the high density of hole traps caused by oxygen vacancies in stoichiometric GeO_x films.

The dielectric constant of pure Ge is 16. The permittivity of tetragonal GeO_2 is evaluated of 12–15.[14] Thus, ε_0 of intermediate germania GeO_x is expected to be between 12 and 16. Low ε_0 value of 4–5 for non-PDA films does not match the expectations. However, extremely low dielectric constant values of 4.5–11 of germania films were observed earlier.[15–18] The reason why the dielectric constant values GeO_x do not fall within the expected interval, and ε_0 is increased after annealing, is an open question. It is possible that during PDA treating germania films are recrystallized, and these changes can cause the increase in the dielectric constant.

In summary, this study indicates that the charge carrier sign in GeO_x depends on stoichiometry, that is, on the methods and conditions of MIS device fabrication. Non-stoichiometric GeO_x films exhibit bipolar conductivity, whereas stoichiometric GeO_2 films after post deposition annealing exhibit unipolar electronic conductivity. This study provides a simple and clear method for determining the charge carrier sign.

This work was supported by projects No. 1.13 and 4.18 of the Siberian Branch of the Russian Academy of Sciences and the National Science Council, Taiwan, under Grant No. NSC-100-2923-E-009-001-MY3.

[1]H.-S. Lan, Y.-T. Chen, W. Hsu, H.-C. Chang, J.-Y. Lin, W.-C. Chang, and C. W. Liu, Appl. Phys. Lett. **99**, 112109 (2011).
[2]A. V. Shaposhnikov, T. V. Perevalov, V. A. Gritsenko, C. H. Cheng, and A. Chin, Appl. Phys. Lett. **100**, 243506 (2012).
[3]C.-H. Hsu, J.-S. Lin, Y.-D. He, S.-F. Yang, P.-C. Yang, and W.-S. Chen, Thin Solid Films **519**, 5033 (2011).
[4]P. Broqvist, J. F. Binder, and A. Pasquarello, Appl. Phys. Lett. **94**, 141911 (2009).
[5]L. Lin, K. Xiong, and J. Robertson, Appl. Phys. Lett. **97**, 242902 (2010).
[6]A. S. Ginovker, V. A. Gritsenko, and S. P. Sinitsa, Phys. Status Solidi B **26**, 489 (1974).
[7]F. H. Hielscher and H. M. Preier, Solid-State Electron. **12**, 527 (1969).
[8]D. R. Islamov, V. A. Gritsenko, C. H. Cheng, and A. Chin, Appl. Phys. Lett. **99**, 072109 (2011).
[9]D. R. Islamov, V. A. Gritsenko, C. H. Cheng, and A. Chin, Appl. Phys. Lett. **101**, 032101 (2012).
[10]N. Novikov, V. A. Gritsenko, and K. A. Nasyrov, Appl. Phys. Lett. **94**, 222904 (2009).
[11]Z. A. Weinberg, Solid-State Electron. **20**, 11 (1977).
[12]S. H. Lin, C. H. Cheng, W. B. Chen, F. S. Yeh, and A. Chin, IEEE Electron Device Lett. **30**, 999 (2009).
[13]K. A. Nasyrov and V. A. Gritsenko, J. Appl. Phys. **109**, 093705 (2011).
[14]A. Kahan, J. W. Goodrum, R. S. Singh, and S. S. Mitra, J. Appl. Phys. **42**, 4444 (1971).
[15]S. Spiga, C. Wiemer, G. Tallarida, G. Scarel, S. Ferrari, G. Seguini, and M. Fanciulli, Appl. Phys. Lett. **87**, 112904 (2005).
[16]M. Kobayashi, G. Thareja, M. Ishibashi, Y. Sun, P. Griffin, J. McVittie, P. Pianetta, K. Saraswat, and Y. Nishi, J. Appl. Phys. **106**, 104117 (2009).
[17]H. Matsubara, T. Sasada, M. Takenaka, and S. Takagi, Appl. Phys. Lett. **93**, 032104 (2008).
[18]R. Xie, W. He, M. Yu, and C. Zhu, Appl. Phys. Lett. **93**, 073504 (2008).